AD-A116 104 NAVAL RESEARCH LAB WASHINGTON DC F/G 17/9
A COMPARISON OF NONCOHERENT AND COHERENT MTI'S.(U)
JUN 82 F F KRETSCHMER, F C LIN, B L LEWIS
UNCLASSIFIED NRL-8591 NL

END
DATE FILMED
08-82
DTIC

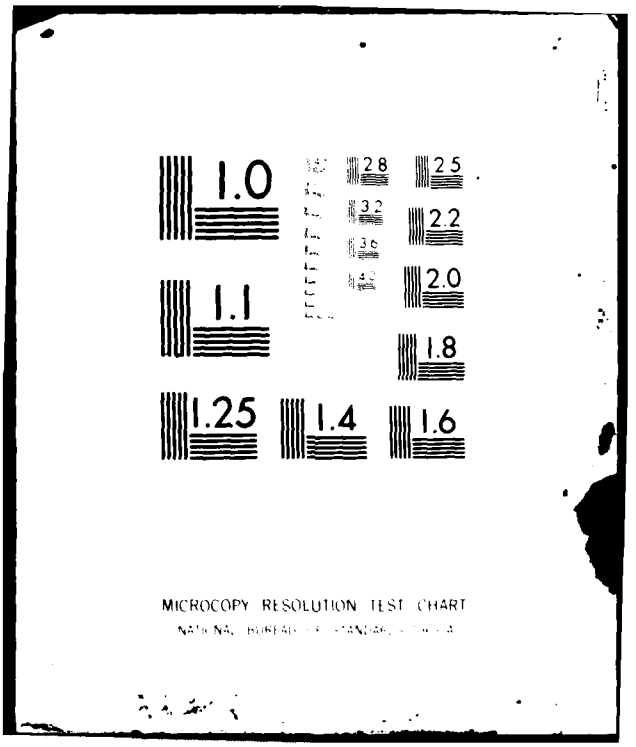
1.0
1.1
1.25
1.4
1.6
2.0
2.2
2.5
1.8
MICROCOPY RESOLUTION TEST CHART

NRL Report 8591

A Comparison of Noncoherent and Coherent MTI's

F. F. KRETSCHMER, JR., F. C. LIN, AND B. L. LEWIS

Target Characteristics Branch
Radar Division

June 22, 1982

NAVAL RESEARCH LABORATORY
Washington, D.C.

SECURITY CLASSIFICATION OF THIS PAGE (When Data Entered)

REPORT DOCUMENTATION PAGE	READ INSTRUCTIONS BEFORE COMPLETING FORM
1. REPORT NUMBER NRL Report 8591	2. GOVT ACCESSION NO. AD-A116 204	3. RECIPIENT'S CATALOG NUMBER
4. TITLE (and Subtitle) A COMPARISON OF NONCOHERENT AND COHERENT MTI's		5. TYPE OF REPORT & PERIOD COVERED An interim report on one phase of the problem
		6. PERFORMING ORG. REPORT NUMBER
7. AUTHOR(s) F. F. Kretschmer, Jr., F. C. Lin, and B. L. Lewis		8. CONTRACT OR GRANT NUMBER(s)
9. PERFORMING ORGANIZATION NAME AND ADDRESS Naval Research Laboratory Washington, DC 20375		10. PROGRAM ELEMENT, PROJECT, TASK AREA & WORK UNIT NUMBERS 62712N SF12-131-691 53-0605-0-2
11. CONTROLLING OFFICE NAME AND ADDRESS Naval Sea Systems Command Washington, DC 20362		12. REPORT DATE June 22, 1982
		13. NUMBER OF PAGES 13
14. MONITORING AGENCY NAME & ADDRESS(if different from Controlling Office)		15. SECURITY CLASS. (of this report) UNCLASSIFIED
		15a. DECLASSIFICATION/DOWNGRADING SCHEDULE

16. DISTRIBUTION STATEMENT (of this Report)

Approved for public release; distribution unlimited.

17. DISTRIBUTION STATEMENT (of the abstract entered in Block 20, if different from Report)

18. SUPPLEMENTARY NOTES

19. KEY WORDS (Continue on reverse side if necessary and identify by block number)

MTI
Coherent MTI
Noncoherent MTI
Radar

20. ABSTRACT (Continue on reverse side if necessary and identify by block number)

Analysis and Monte Carlo simulations reveal that a noncoherent MTI using an envelope detector differs from one using a square law detector. The square law detector is usually considered because of ease of analysis, and it is commonly stated or implied that the results are the same because of the similar spectral characteristics of the detectors. A comparison is made between the two noncoherent MTI's and the coherent MTI in terms of clutter attenuation and MTI improvement factors.

DD FORM 1 JAN 73 1473 EDITION OF 1 NOV 65 IS OBSOLETE
S/N 0102-014-6601

SECURITY CLASSIFICATION OF THIS PAGE (When Data Entered)

CONTENTS

A COMPARISON OF NONCOHERENT AND COHERENT MTI's

INTRODUCTION

Noncoherent moving target indication (MTI) differs from coherent MTI in that the MTI processing is performed at video after an envelope or square law detector [1-5]. In the coherent MTI, processing is done at IF or more commonly in the complex video inphase I and quadrature Q channels.

The noncoherent MTI is similar in many ways to the coherent MTI but differs in some important respects. With the noncoherent MTI, if the pulse-to-pulse changes in the amplitude of the clutter return are small, the clutter will be heavily attenuated by the MTI filter following the envelope detector. Since the phase of the clutter is not used, the noncoherent MTI is capable of centering the cancellation notch on clutter having a nonzero average radial velocity. In the presence of clutter, a target having a different radial velocity from that of the clutter will cause pulse-to-pulse amplitude variations and the target plus clutter signal will not be as heavily attenuated by the MTI filter. Since the target signal is clutter referenced it will be canceled in the absence of clutter unless the target scintillates.

An examination of the existing literature indicated that little analytical work has been performed on the noncoherent MTI, particularly based on the envelope detector which is of interest in this report. Prior work [3,4] considered the envelope detector to behave approximately as a square law detector and based the results on arguments relating to the spectral characteristics of the clutter signal after a square law detector.

In this report, a statistical approach is taken, in both the analysis and the Monte Carlo simulations, which is not based on any spectral approximations. Clutter attenuation and improvement factors based on generalized definitions are computed and compared to the coherent MTI.

It is shown that the common assumption that the clutter standard deviation is increased by a factor of $\sqrt{2}$ is not valid for the noncoherent MTI using an envelope detector for values of the correlation coefficient which are required for good MTI performance. The factor of $\sqrt{2}$ spectral spread is attributed by other investigators to the alleged square law behavior of the envelope detector which results in a self-convolution of the clutter power spectral density which exists prior to the envelope detector.

COMPARISON OF COHERENT AND NONCOHERENT MTI

Coherent MTI

First we consider the clutter attenuation for a two-pulse coherent MTI. The successive clutter returns are designated by the complex video vectors consisting of the I and Q values, or equivalently the amplitude and phase which are computed from $(I^2 + Q^2)^{1/2}$ and $\tan^{-1}(Q/I)$ respectively.

For a two-pulse canceler the complex residue signal is

$$R = C_1 - C_2 \tag{1}$$

where C_1 and C_2 are successive complex clutter return signals from a given range cell separated in time by the interpulse period T.

Manuscript submitted February 17, 1982.

The average residue power C_0 is taken to be

$$\begin{aligned} C_0 = \overline{|R|^2} &= \overline{|C_1 - C_2|^2} \\ &= \overline{(C_1 - C_2)(C_1 - C_2)^*} \\ &= \overline{|C_1|^2} + \overline{|C_2|^2} - 2\mathrm{Re}\,\overline{C_1 C_2^*}. \end{aligned} \tag{2}$$

The cross correlation term $\mathrm{Re}\,\overline{C_1 C_2^*}$ may be determined from the I and Q components

$$\begin{aligned} \mathrm{Re}\,\overline{C_1 C_2^*} &= \mathrm{Re}\,\overline{(C_{1I} + jC_{1Q})(C_{2I} - jC_{2Q})} \\ &= \overline{C_{1I} C_{2I}} + \overline{C_{1Q} C_{2Q}} = 2\rho\sigma^2 \end{aligned} \tag{3}$$

where it is assumed that the I and Q components of each clutter return have the same variance σ^2 and each have the same correlation coefficient ρ. Substituting Eq. (3) in Eq. (2) results in

$$C_0 = \overline{|R|^2} = 4\sigma^2 - 4\rho\sigma^2 = 4\sigma^2(1 - \rho). \tag{4}$$

Letting the input clutter power be

$$C_{in} = \overline{|C_1|^2} = \overline{|C_2|^2} = 2\sigma^2, \tag{5}$$

the clutter attenuation or cancellation ratio is

$$CR = \frac{C_{in}}{C_0} = \frac{1}{2(1 - \rho)}. \tag{6}$$

This result may be generalized in terms of matrix notation as follows. Let W denote the column matrix of weights applied to the successive clutter samples C_i and let M_c denote the covariance matrix of the clutter which is given by

$$M_c = \overline{CC^t} \tag{7}$$

where C^t denotes the complex conjugate of the transposed matrix C. Letting T denote the transpose operation, the residue power is

$$\begin{aligned} C_0 &= \overline{(W^T C)(W^T C)^t} \\ &= \overline{W^T C\, C^t W^*} = W^T M_c W^*. \end{aligned} \tag{8}$$

Applying Eq. (8) to the two-pulse canceler example described above, we have

$$C_0 = (1 \; -1) \begin{pmatrix} 2\sigma^2 & 2\sigma^2\rho \\ 2\sigma^2\rho & 2\sigma^2 \end{pmatrix} \begin{pmatrix} 1 \\ -1 \end{pmatrix} = 4\sigma^2(1 - \rho)$$

which agrees with Eq. (4).

The clutter cancellation ratio may be expressed in general form as

$$CR = \frac{2\sigma^2}{W^T M_c W^*}. \tag{9}$$

The MTI improvement factor I is determined by the ratio of the output target-to-clutter ratio divided by the input target-to-clutter ratio where the input target is averaged over all velocities if no a priori knowledge is available. The average target response, or target enhancement factor, is equivalent to normalizing the filter response to white noise so that the output noise power is equal to the input noise power. It follows that

$$I = \frac{\overline{T_0/C_0}}{T_{in}/C_{in}} = \overline{\left(\frac{T_0}{T_{in}}\right)}\left(\frac{C_{in}}{C_0}\right)$$

$$= (W^T W^*) \cdot (CR) = \frac{2\sigma^2 (W^T W^*)}{W^T M_c W^*} \tag{10}$$

where we have made use of Eq. (9) and the fact that the white noise response of the filter is given by $W^T W^*$.

Noncoherent MTI

For the two-pulse noncoherent MTI, the output clutter residue is

$$R = |C_1| - |C_2| \tag{11}$$

and the output clutter power is

$$C_0 = \overline{R^2} = \overline{(|C_1| - |C_2|)^2} \tag{12}$$

$$= \overline{|C_1|^2} + \overline{|C_2|^2} - 2\overline{|C_1||C_2|}.$$

From Refs. 6 to 8 the cross-correlation term is given by

$$\overline{|C_1||C_2|} = 2\sigma^2 \frac{\pi}{4} {}_2F_1\,(-1/2,\ -1/2,\ 1,\ \rho^2) \tag{13}$$

where ${}_2F_1\,(a,\ b,\ c,\ x)$ is the Gaussian hypergeometric function [6] given by

$${}_2F_1(a,\ b,\ c,\ x) = 1 + \frac{ab}{c1!}x + \frac{a(a+1)b(b+1)}{c(c+1)2!}x^2 \ldots .$$

In particular, we have

$${}_2F_1\,(-1/2,\ -1/2,\ 1,\ \rho^2) = 1 + \frac{1}{4}\rho^2 + \frac{1}{64}\rho^4 + \frac{1}{256}\rho^6 + \ldots . \tag{14}$$

References 6 to 8 use an identity given in Ref. 9 as

$${}_2F_1\,(-1/2,\ -1/2,\ 1,\ \rho^2) = \frac{4}{\pi} E(\rho) - \frac{2}{\pi}(1-\rho^2)\,K(\rho) \tag{15}$$

where K and E are complete elliptic integrals of the first and second kinds respectively. These functions are tabulated in Ref. 10 and are also available as a subroutine on the NRL ASC digital computer where they are defined in terms of ρ^2 and are designated as $E(\rho^2)$ and $K(\rho^2)$. Incorrect usage of these tabulated values leads to erroneous results. To be consistent with the literature we retain the notation of $E(\rho)$ and $K(\rho)$.

From Eqs. (12), (13), and (15), the resultant output clutter is

$$C_0 = 4\sigma^2\,[1 - \pi/4\ \ {}_2F_1\,(-1/2,\ -1/2,\ 1,\ \rho^2)]$$

$$= 4\sigma^2\left[1 - \left\{E(\rho) - \frac{(1-\rho^2)}{2}\,K(\rho)\right\}\right] \tag{16}$$

which may be written more compactly as

$$C_0 = 4\sigma^2[1 - F(\rho)] \tag{17}$$

where

$$F(\rho) = \frac{\pi}{4} {}_2F_1\,(-1/2,\ -1/2,\ 1,\ \rho^2)$$

$$= E(\rho) - \left(\frac{1-\rho^2}{2}\right) K(\rho). \tag{18}$$

Comparison of Eq. (17) with the expression for the coherent MTI in Eq. (4) shows the expressions are the same if one interchanges ρ and $F(\rho)$. This result generalizes for higher order cancelers so that for the noncoherent canceler the output clutter may be expressed in a similar way to Eq. (8) as

$$C_0 = W^T M_N W^* \tag{19}$$

where M_N is the covariance matrix of the noncoherent MTI which is the same as M_c in Eq. (8) except that ρ is replaced by $F(\rho)$. In either case, it is noted that ρ is a function of time separation which is equal to the Fourier transform of the clutter power spectral density and is dependent on the interpulse intervals.

From the previous results, the cancellation ratio for the noncoherent MTI is given by

$$CR = \frac{2\sigma^2}{W^T M_N W^*}. \tag{20}$$

A discussion of the improvement factor for the noncoherent MTI is deferred to later in this section.

Comparison of Cancellation Ratios

At this juncture, we compare the cancellation ratios of the coherent and noncoherent MTI for a clutter spectrum which is assumed to be Gaussian and given by

$$G(f) = \frac{1}{\sqrt{2\pi}\sigma_s} e^{-f^2/2\sigma_s^2} \tag{21}$$

where σ_s denotes the standard deviation of the clutter spectrum. The correlation function $\rho(\tau)$ is the Fourier transform of $G(f)$ and is given by

$$\rho(\tau) = e^{-2\pi^2(\sigma_s\tau)^2} \tag{22}$$

where τ is the time delay variable.

A useful relationship for the Gaussian spectrum is that

$$\rho(k\tau) = [\rho(\tau)]^{k^2}. \tag{23}$$

By use of Eq. (8) and Eqs. (20) through (23), the cancellation ratio was computed for the coherent and noncoherent MTI and the results are shown in Fig. 1 for various order cancelers where the standard binomial weighting was used. In Fig. 1 the abscissa denotes the spectral width σ_s which is normalized to the pulse repetition frequency (prf). Figure 1(a) shows the comparison for the two- and three-pulse cancelers, and Fig. 1(b) shows the comparison for the four- and five-pulse cancelers.

For the two-pulse canceler, it is shown that the noncoherent MTI is approximately 3 dB better than the coherent MTI in contrast to prior beliefs. Skolnik [1] noted this result by use of a simple vector relationship. A more detailed derivation using vectors is given in the appendix. For higher order cancelers the noncoherent clutter attenuation is seen in Fig. 1 to be generally worse than the coherent MTI except for the three-pulse canceler whose curves cross over for σ_s/prf approximately equal to 0.07.

The clutter attenuation of the coherent and noncoherent MTI's was also simulated on a digital computer using Monte Carlo techniques, which are described later, and excellent agreement was obtained.

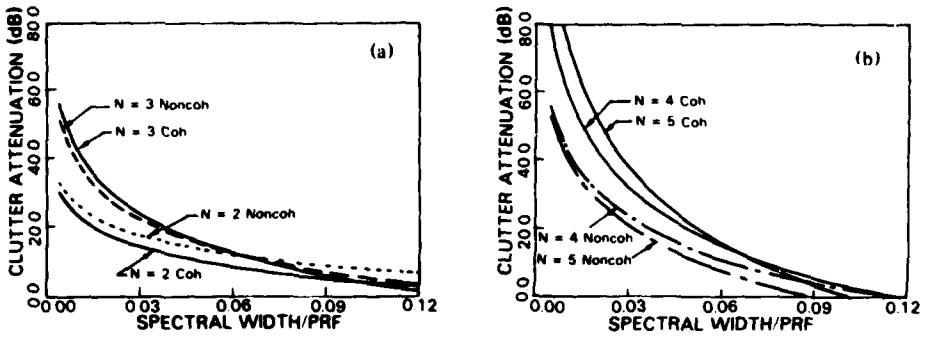

Fig. 1 — Clutter attenuation of coherent and noncoherent (envelope detector) MTI's. (a) 2- and 3-pulse canceler and (b) 4- and 5-pulse canceler.

At first glance, it may appear strange that the clutter attenuation curves for the coherent MTI cross over as shown in Fig. 1. However, since the improvement factor given in Ref. 10 asymptotically approaches unity the clutter attenuation cannot become less than the reciprocal of the target enhancement factor. This also follows from the relation

$$\lim_{\rho \to 0} CR = \lim_{\rho \to 0} \frac{2\sigma^2}{W^T M_c W^*} = \frac{2\sigma^2}{2\sigma^2 W^T W^*} = \frac{1}{W^T W^*} \tag{24}$$

where we have made use of the fact that M_c approaches $2\sigma^2$ times the identity matrix as ρ approaches 0.

Spectral Spreading Evaluation

Next, we examine the relationship between the coherent and noncoherent cancelers in terms of a spectral spreading factor. That is, for a given σ_s/prf in Fig. 1 and the associated noncoherent clutter attenuation, we find the multiplicative factor for σ_s/prf which results in the corresponding coherent canceler having the same cancellation ratio as the noncoherent canceler.

This is plotted in Fig. 2 where it is seen that there is no simple relationship which may be stated in regard to the spectral spreading factor.

It was previously shown that the clutter output power of the coherent or noncoherent MTI filters can be computed from Eqs. (8) or (19), where the difference lies in the covariance matrices M_c and M_N. As previously described, the difference between the matrices is that ρ in the coherent covariance matrix is replaced by $F(\rho)$ given by Eqs. (18) and (14) as

$$F(\rho) = \frac{\pi}{4} {}_2F_1\left(-1/2, -1/2, 1, \rho^2\right).$$

$$= \frac{\pi}{4}\left[1 + \frac{\rho^2}{4} + \frac{\rho^4}{64} + \frac{\rho^6}{256} + \ldots\right].$$

From this expansion several observations may be made. First, the envelope detector corresponds to an expansion in even powers of ρ. Also, the only term which can be identified with a square law detector is the ρ^2 term, which corresponds to a convolution of the power spectral densities in the frequency domain. It is found that in the region of interest where good MTI performance is obtained, ρ is nearly unity and even using as many as the first three terms of the expansion yields inaccurate results for the envelope detector case. Note that the spectrum corresponding to $F(\rho)$ consists of a summation

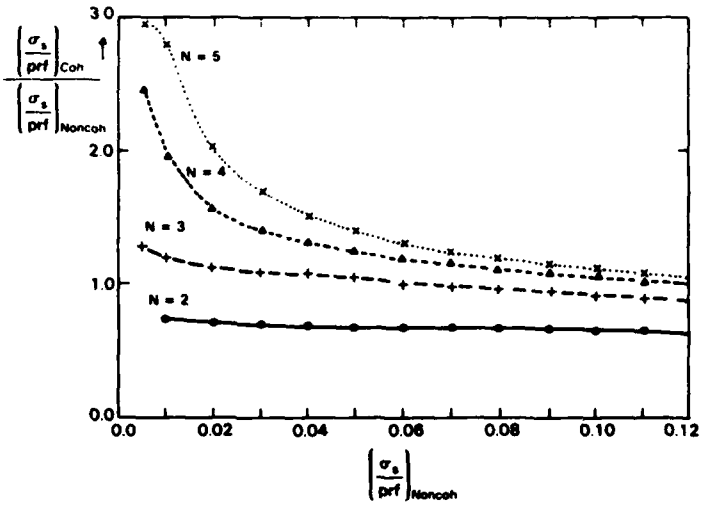

Fig. 2 — Spectral spreading factor for noncoherent MTI using an envelope detector

of Gaussian terms having unequal variances and that the resultant spectrum is non-Gaussian, in contrast to the output spectrum of the square law detector. Hence, the spectral spreading factor is an equivalence only in terms of the resultant value of the cancellation ratio.

Improvement Factor Comparison

Because of the nonlinearity of the envelope detector in a noncoherent MTI system it is not appropriate to separately determine the doppler-averaged target response and the clutter attenuation and combine these factors as was discussed for the coherent MTI whose improvement factor was given by Eq. (10). To circumvent this problem we define the output target-to-clutter power ratio as

$$\frac{T_0}{C_0} = \frac{(T+C)_0 - C_0}{C_0}. \tag{25}$$

The improvement factor using the generalized definition becomes

$$I = \frac{\overline{(T+C)_0 - C_0}}{T_{in}} \frac{C_{in}}{C_0} \tag{26}$$

where the averaging is over all target velocities.

Due to the nonlinearity of the noncoherent MTI, the improvement factor will in general be dependent on the input target-to-clutter ratio. In Ref. 7 an approximate relationship is derived which gives the value of $\overline{|C_1||C_2|}$, needed for the noncoherent MTI, for the small target-to-clutter ratio. However, this relation was found to be unsatisfactory since for a zero target-to-clutter ratio the expression reduces to the expression containing the first three terms of the Gaussian hypergeometric function which is not sufficiently accurate for values of ρ near unity. Therefore, computer simulations were performed using Monte Carlo techniques. For the different order cancelers successive clutter samples,

corresponding to the returns from a given range cell on successive sweeps, were generated on the computer. The correlation between successive sweeps was specified, and the MTI residue was computed for each trial consisting of N sweeps for an N-pulse MTI. Three thousand independent trials were run, and the residues were averaged for each case.

On each trial the first return was taken to have a Rayleigh distributed amplitude and a uniformly distributed phase, and successive returns were correlated with the first return. This was achieved as follows. The first clutter sample was generated from two independent Gaussian distributions associated with the I and Q components of C_1, with each distribution having a mean of 0 and a variance equal to σ^2. The next clutter sample was obtained from a distribution C_2' which had a correlation of $\rho(T)$ with C_1. For a three-pulse canceler, for example, a third clutter sample was taken from the distribution C_3' which had a correlation $\rho(T)$ with C_2' and $\rho(2T)$ with C_1 which we renamed C_1'. Thus in the primed coordinates the distributions are mutually correlated complex Gaussian distributions that are normalized to have zero mean and a variance of σ^2 in both the I and the Q components.

The above remarks may be summarized in mathematical terms for the three-pulse example as

$$\begin{aligned} C_1' &= a_{11}\, C_1 \\ C_2' &= a_{21}\, C_1 + a_{22}\, C_2 \\ C_3' &= a_{31}\, C_1 + a_{32}\, C_2 + a_{33}\, C_3 \end{aligned} \tag{27}$$

where

$$\begin{aligned} a_{11} &= 1, & a_{22} &= [1 - \rho^2(T)]^{1/2}, \\ a_{21} &= \rho(T), & a_{32} &= \rho(T)\frac{[1 - \rho\,(2T)]}{a_{22}}, \\ a_{31} &= \rho(2T), & a_{33} &= [1 - \rho^2(2T) - a_{32}^2]^{1/2}. \end{aligned}$$

The MTI was then simulated by applying the binomial weighting to the complex C_i' samples, or to the amplitude of the C_i' samples, for the coherent and noncoherent cases respectively. For different values of $\rho(T)$, 3000 independent trials were run and the output residue powers were averaged. The cancellation ratios were computed for the two cases, where the input clutter power for each was taken as the average of the input $(I^2 + Q^2)$ value which is $2\sigma^2$. The output clutter power for the coherent case was taken as the average residue, again computed from $(I^2 + Q^2)$, averaged over the 3000 independent trials. The noncoherent residue power was computed by averaging the square of the residue. Thus, both systems are computed with common input and output terminals.

The target signal was added to the clutter signal with a random initial phase angle and a specified phase shift corresponding to the target's doppler. The average target output power as determined from the generalized definition (Eq. (25)) was determined for 10 different target velocities uniformly spaced across the prf interval. Excellent agreement was obtained with the known improvement factor for the coherent MTI case. The results for the coherent and noncoherent MTI are plotted in Fig. 3 for an input clutter-to-target ratio of 20 dB. The results were nearly the same for all clutter-to-target ratios above 10 dB. It is seen that the improvement factors for the two-pulse canceler are nearly the same while the noncoherent MTI improvement factor degrades relative to the coherent MTI as the number of pulses increases. A comparison with the improvement factor computed from the relation in Steinberg [3], for a square law device, is shown in Fig. 4 where it is seen that the improvement factor for the square law detector is equal to or greater than that for the envelope detector. In Fig. 5, the target enhancement factor of the simulated noncoherent MTI is compared with the coherent MTI for a clutter-to-target ratio of 20 dB. It is seen that the noncoherent MTI target enhancement factor is approximately 3 dB less than that for the coherent MTI.

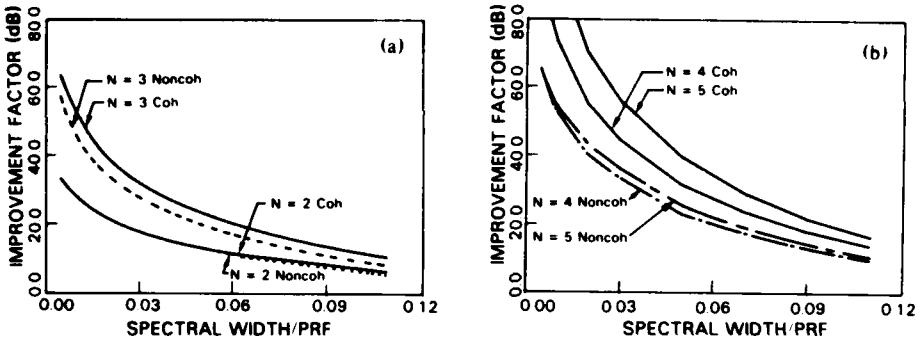

Fig. 3 — Improvement factors of coherent and noncoherent (envelop detector) MTI's. (a) 2- and 3-pulse canceler and (b) 4- and 5-pulse canceler.

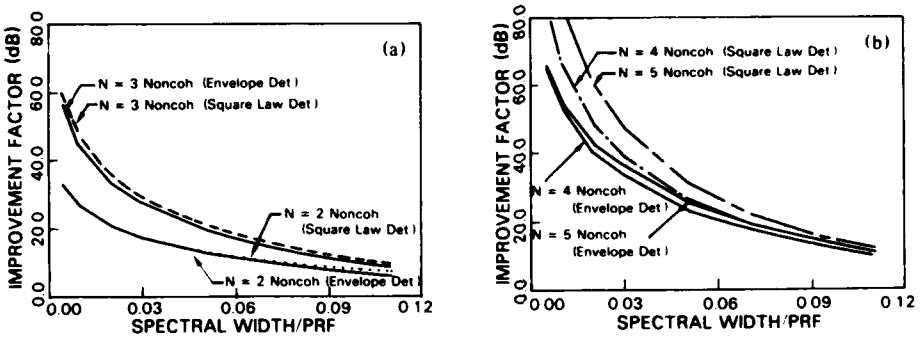

Fig. 4 — Improvement factors for noncoherent MTI's using an envelope and a square law detector. (a) 2- and 3-pulse canceler and (b) 4- and 5-pulse canceler.

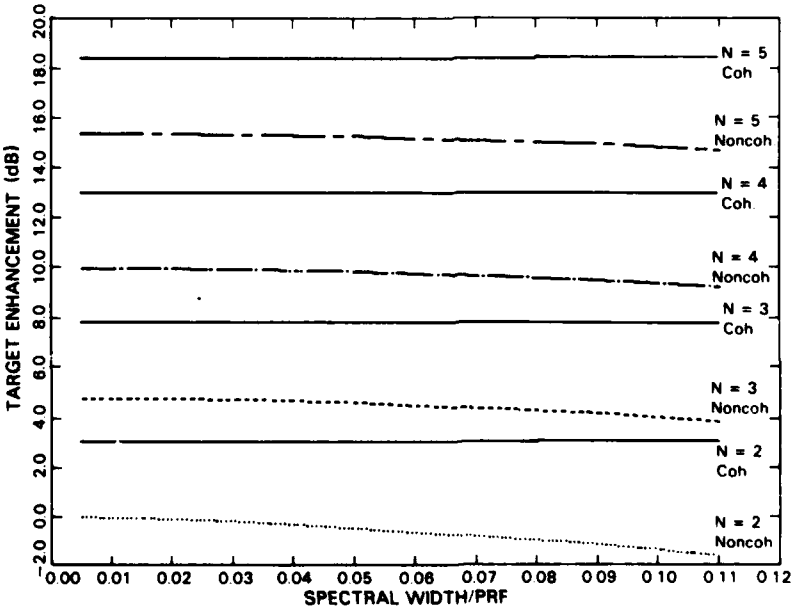

Fig. 5 — Target enhancement factor vs normalized spectral width for coherent MTI and noncoherent MTI using an envelope detector

SUMMARY AND CONCLUSIONS

A comparison between a coherent MTI and a noncoherent MTI using an envelope detector has been made based on statistical analysis and on computer simulations using Monte Carlo techniques. This approach differs from prior investigations which base the results on the envelope detector behaving approximately as a square law detector from which it is argued that the standard deviation of the power spectral density of the clutter is increased by $\sqrt{2}$ due to the self-convolution of the clutter spectra.

The results of the analysis in this report indicate that in general, the envelope detector cannot be regarded as a square law detector which increases the standard deviation of the clutter spectrum by $\sqrt{2}$. The equivalent spectral spread was found to depend on the number of pulses used in the MTI as well as on the correlation of the returned clutter signals. It was noted that the spectrum after envelope detection is not Gaussian since the correlation function consists of higher order terms than ρ^2 which cannot be ignored. Thus, the equivalent spectral spreading of the input Gaussian clutter spectrum prior to envelope detection is an equivalency only in terms of the value of the cancellation ratio. It was also found that the clutter attenuation for the two-pulse noncoherent canceler using an envelope detector is 3 dB better than the clutter attenuation for the coherent canceler in contrast to some prior conceptions.

In terms of improvement factors, it was found that the two noncoherent MTI's and the coherent MTI are nearly the same for the two-pulse canceler. As the number of pulses increases, the improvement factors become more unequal. The coherent MTI has the largest improvement factor, followed in order by the square-law and envelope detector MTI's.

REFERENCES

1. M.I. Skolnik, *Introduction to Radar Systems*, McGraw-Hill, New York, 1962.

2. F.E. Nathanson, *Radar Design Principles*, McGraw-Hill, New York, 1969.

3. B.D. Steinberg, in *Modern Radar Analysis, Evaluation and System Design*, R.S. Berkowitz, ed., John Wiley and Sons, New York, 1965, Chaps. 1 and 2, Part IV.

4. D.C. Schleher, ed., *MTI Radar*, ARTECH House, 1978.

5. R.C. Emerson, "Some Pulsed Doppler MTI and AMTI Techniques." (This paper appears in Ref. 4.)

6. D. Middleton, *An Introduction to Statistical Communication Theory*, McGraw-Hill, New York, 1960.

7. J.L. Lawson and G.E. Uhlenbeck, eds., *Threshold Signals*, MIT Radiation Lab. Series 24, McGraw-Hill, New York, 1950.

8. W.B. Davenport, Jr., and W.L. Root, *An Introduction to the Theory of Random Signals and Noise*, McGraw-Hill, New York, 1958.

9. W. Magnus and F. Oberhettinger, *Special Functions of Mathematical Physics*, Chelsea, New York, 1949.

10. M. Abramowitz and I.A. Stegun, eds., *Handbook of Mathematical Functions*, National Bureau of Standards, 1964.

Appendix

APPROXIMATE CLUTTER RESIDUES FOR A TWO-PULSE CANCELER USING VECTOR RELATIONS

Letting C_1 and C_2 denote independent complex Gaussian variables having 0 mean and a variance of σ^2 for the I and Q components, we make the linear transformation

$$C_1' = C_1$$
$$C_2' = \rho C_1 + (1-\rho^2)^{1/2} C_2 = \rho C_1 + dC_2 \tag{A1}$$

where $d = (1-\rho^2)^{1/2}$. Then C_1' and C_2' are also Gaussian random variables whose correlation is ρ and whose mean and variance are the same as for C_1 and C_2.

We next consider the residue vector of a two-pulse coherent MTI given by

$$R = C_1' - C_2'. \tag{A2}$$

These relations are shown in Fig. A1. The average residue power using Eqs. (A1) and (A2) is then

$$\overline{|R|^2} = (1-\rho)^2 \overline{|C_1|^2} + d^2 \overline{|C_2|^2}.$$

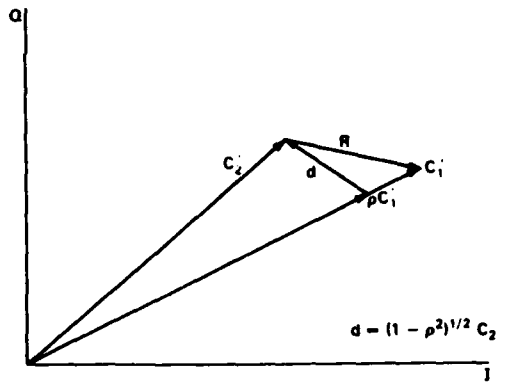

Fig. A1 — 2-pulse MTI vector relations

Letting $\rho = 1 - \epsilon$, it is seen that the term

$$(1-\rho)^2 = [1-(1-\epsilon)]^2 = \epsilon^2$$

which is small compared to the term

$$d^2 = (1-\rho^2) \approx 2\epsilon$$

so that

$$\overline{|R|^2} = 2\epsilon(2\sigma^2) = 4\sigma^2(1-\rho) \tag{A3}$$

in agreement with Eq. (4).

For the noncoherent MTI the term dC_2 may be regarded as being composed of inphase and quadrature components relative to C_1' and since the orthogonal component contributes little to the amplitude of C_2', we approximate the vector length of C_2' as

$$\overline{|C_2'|} = \rho|C_1| + \frac{d}{\sqrt{2}}|C_2|$$

so that

$$\overline{R^2} = \overline{(|C_1'| - |C_2'|)^2} = \left[(1-\rho)^2 + \frac{d}{2}\right]^2 2\sigma^2$$

which, using the previous approximations may be written as

$$\overline{R^2} \approx \frac{d^2}{2}(2\sigma^2) \approx \epsilon 2\sigma^2. \tag{A4}$$

Comparison of Eqs. (A3) and (A4) shows that the residue clutter power of the two-pulse noncoherent MTI is 3 dB less than that for the coherent MTI.


DATE
FILMED
8-8